Proc. Indian Acad. Sci. (Chem. Sci.), Vol. 112, No. 3, June 2000, pp. 311–322

Fluorescence metrology of silica sol–gels – The effect of D_2O and inorganic salts

D J S BIRCH* and C D GEDDES
Photophysics Group, Department of Physics and Applied Physics, University of Strathclyde, 107 Rottenrow, Glasgow, G4 ONG, UK
e-mail: djs.birch@strath.ac.uk

Abstract. We have developed a new method for measuring *in-situ* the growth of the nanometre-size silica particles which lead to the formation of sol–gel glasses. This technique is based on the decay of fluorescence polarisation anisotropy due to Brownian rotation of dye molecules bound to the particles. Results to date give near ångstrom resolution and demonstrate the feasibility of the approach both for providing industrial quality control and helping fundamental research. Our approach has several key advantages over traditional techniques for nanometre metrology, such as small angle X-ray and neutron scattering and electron microscopy. In this paper we present silica particle growth dynamics in a hydrogel as detected by two near-infrared dyes, the effect of adding D_2O on the hydrodynamic radius and the effect of salt addition.

Keywords. Fluorescence anisotropy; sol–gel; particle size; syneresis.

1. Introduction

Sol–gel glasses find many important applications ranging from everyday applications of silica gel in cleaning, polishing, brewing, printing and adhesive agents to applications in photonics and sensors. These represent multi-million pound industries worldwide, all being potential benefactors of a better understanding of the underlying science and monitoring of the industrial processes.

Over the past two decades the picture has emerged that sol–gel glasses are formed by the coalescence of nanometre scale (SiO_2) particles rather than by the extension and cross-linking of polymer chains as is the case for organic polymers[1]. The sol–gel process is a room temperature inorganic polymerisation involving a series of hydrolysis and condensation steps whereby a colloidal suspension (sol) changes into a rigid network (gel), and which owes its origins to the pioneering work of Ebelman, Mendeleyev and Graham in the 19th century. More recently, sol–gel technology has found a renaissance in photonics, for example, as the process responsible for GRIN (graded refractive index) lens fabrication. The sol to gel transition is characterised by a gel point, after a time t_g, at which a fine silica network spans the containing vessel, although most of the volume is still in the fluid phase at t_g. Of all the possible syntheses, sodium silicate (i.e. water glass) production of silica gel, through the addition of sulphuric acid to control *p*H and the formation of siloxane (–Si–O–Si–) bonds, has the greatest industrial significance. This is due to the large-scale production of silica gel for everyday general use as an absorptive,

---

*For correspondence

abrasive, carrying and surface coating agent. Therefore, given their industrial importance, it is perhaps somewhat surprising that silica particle dynamics in hydrogels have received so little attention in the research literature. Undoubtedly, this is in part due to the difficulty of *in-situ* measurements of sufficient resolution in the early stages of polymerisation, when ~ 1 nm to 5 nm particles exist, and after t_g when the silica gel matrix distorts small-angle scattering measurements. The situation is further complicated because the very word 'particle' implies a Newtonian solid description of what, apart from the very late stages of gelation, is probably a much more open, hydrated and ramified structure.

Different sol–gel processes are used to fabricate photonic devices and are frequently based on alcogel preparations from silicon alkoxides such as tetramethoxysilane dissolved in methanol. Alkoxide preparations have a better defined constituent structure than silica hydrogels and hence the dynamics of formation have been more widely studied. In this paper we concentrate on metrology in silica hydrogels, although the technique we propose, can in principle, be customised for any kind of sol–gel.

For both the sol–gel preparations mentioned above, there is a similar gel network forming step i.e. the condensation reaction:

$$\equiv\mathrm{Si{-}OH} + \mathrm{OH{-}Si}\equiv \;\rightarrow\; \equiv\mathrm{Si{-}O{-}Si}\equiv + \mathrm{H_2O}. \tag{1}$$

Brinker and Scherer[1] have outlined the effect of pH and surface charge on t_g and particle growth. At $p\mathrm{H} \approx 2$ the surface charge is neutral, becoming slightly positive at $p\mathrm{H} < 2$ (acidic gels), resulting in long gel times and particle growth largely through aggregation up to ≈ 4 nm. The surface charge is negative at $p\mathrm{H} > 2$, facilitating more rapid gelation up to pH 6. At $p\mathrm{H} > 7$ alkaline silicate liquors contain highly anionic particles, which are mutually repulsive, form stable and non-gelling sols and can grow to many tens of nanometres, mainly by the dissolution of smaller particles and deposition of silica on larger particles due to solubility differences (Ostwald ripening). As silica particles join to form a gel, voids filled with solvent are formed between the particles, the size of these being related to the particle mean size. As a gel is dried and then broken up to give the fine silica gel powders used in many applications (e.g. chromatography, toothpaste etc) the particle size determines the surface area, which is a key parameter controlling the product performance (e.g. adsorption efficiency in chromatography, protein extraction in beer fining etc.). Very large internal surface areas can be formed by the sol–gel process. For example, 1 g of gel can have the equivalent surface area to a 25 m swimming pool. A smaller particle size leads to an increased gel surface area and hence by controlling pH (e.g. by adding sulphuric acid in the case of silica hydrogels) the surface area of the silica end-product can be controlled. At present there is no on-line monitoring of the particle size during industrial production which could lead to feedback control of the surface area and porosity of the silica end-product. Successful development of the ideas we are developing could overcome this deficiency.

Moreover, considerable theoretical effort has been applied to finding solutions of diffusion equations and computer simulations in order to model silica cluster growth[1]. Ultimately, the applicability of such models can only be tested and developed through accurate size measurements.

Small angle X-ray and neutron scattering are the traditional techniques used for nm particle size measurement in silica sols[1]. Unlike fluorescence anisotropy metrology, which we describe here, scattering techniques provide no viscosity information. Also, because fluorescence anisotropy decay selectively detects dye bound to rotating particles as against dye bound in the gel matrix, the approach we propose is better placed than scattering techniques for recording particle size *in situ* at high silicate concentrations and after gelation. Scattering occurs from the matrix as well as the particles after gelation and from multiple sites where high particle number densities are studied. Our approach is more suitable for on-line industrial monitoring and is much less expensive. Light scattering has insufficient resolution and although in principle fluorescence correlation spectroscopy[2] and fluorescence recovery after photobleaching[3] (FRAP) have sufficient resolution, they require particle dilution (which produces depolymerisation) and a microscope. Scanning electron microscopy cannot be performed *in-situ* as the sol has to be dried.

We have been seeking to address both the fundamental physics questions concerning the growth dynamics and provide a new method of monitoring the industrial production of sol–gel glasses by means of time-resolved fluorescence measurements on silica particles labelled with a fluorescent dye. Successful implementation of our ideas could translate basic research on particle collision dynamics in sols into improvements in industrial technologies by developing a new approach to nm silica particle metrology.

Changes in the decay of fluorescence anisotropy as polymerisation proceeds are simply explained in terms of changes in the relative abundance of solvated dye and dye attached to silica particles, changes in silica particle size and sol microviscosity, as depicted in figure 1. This dual environment of a dye means that a single anisotropy decay measurement leads to determination of all the important hydrodynamic parameters.

Although fluorescence anisotropy decay due to Brownian rotation is a well established technique for studying areas as disparate as protein folding dynamics and membrane fluidity[4], it has found little if any application to particle size measurement. In fact, as our results show, the fluorescence decay time of most dyes (~1 ns to 10 ns) is ideally compatible with the critical particle size range for sol–gel systems of 1–5 nm.

Recently we have reported the growth dynamics of silica particles for a range of sol compositions and *p*H using the near-infrared dye JA120[5,6]. Here we contrast and compare these findings with those for another near-infrared dye, JA53[7], and investigate the effect of adding D_2O and inorganic salts on the silica particle metrology.

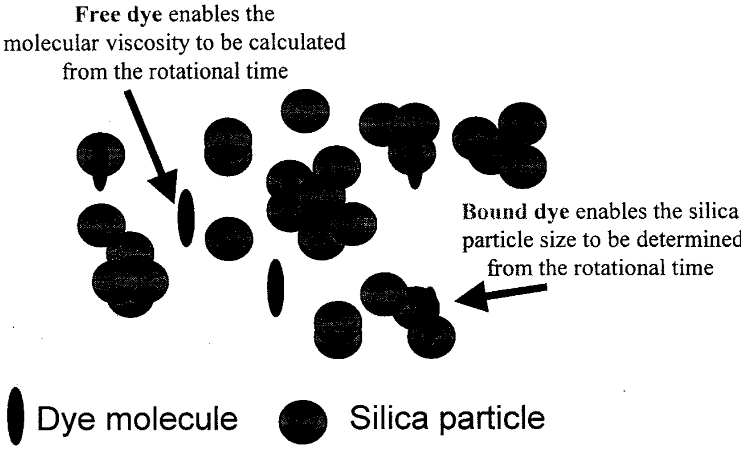

Figure 1. Dye tracking sol–gel microviscosity and silica particle size.

2. Experimental

Fluorescence anisotropy decay measurements were performed using time-correlated single-photon counting[8] (TCSPC). TCSPC has picosecond time-resolution and 10^6 dynamic range as well as offering rapid measurement using high repetition rate (≈MHz) ps diode or fs Ti:sapphire laser excitation. Even low cost pulsed LED ns excitation could be used. Figure 2 shows a schematic diagram of a typical arrangement with which we have obtained our results. Orthogonal, polarised fluorescence decay curves can be recorded in ≈ two minute measurement times at different delay times following initial mixing of the sol. Such rapid measurements are necessary to minimize the effect of the continuously changing sol. In measurements reported here a diode laser was used for excitation and a single photon avalanche diode (SPAD) for detection. The 650 nm diode laser generated 70 mW vertically polarised optical pulses of duration ≈ 50 ps at 1 MHz repetition rate. The overall instrumental response function was ≈ 350 ps fwhm. Fluorescence at 700 nm was selected using a monochromator and/or a cut-off filter and a dichroic or prism polariser. The fluorescence anisotropy decay curves can be analysed to give the decay parameters using the IBH nonlinear least squares impulse reconvolution analysis with a chi-squared, c^2, goodness of fit criterion[8].

The detailed synthetic preparation and titration of silica sols has been described previously[5,6]. Table 1 shows the compositions of sol–gels studied in this paper. Dyes were added to the bulk sol directly after preparation to give concentrations of $\approx 10^{-5}$ mol dm^{-3} and were then cast in 4 cm^3 quartz cuvettes. For D_2O and H_2O sols, 1·5 cm^3 D_2O and 1·5 cm^3 doubly distilled deionised H_2O respectively were added to 1·5 cm^3 of pure sol in 4 cm^3 quartz cuvettes. The t_g values for the sol–gels shown in table 1 were determined by noting the range of times when 1 litre of sol (using the same 1 L Nalgene beaker) had thickened sufficiently to start peeling away from the sides of the beaker to the point when it could no longer flow and had set firm. Obviously for low density sol–gels t_g is broader and greater than for higher density (i.e. greater % w/w SiO_2) sol–gels containing the same excess acid normality. Bulk viscosities were determined, just up to $t_{g,}$, using Ostwald viscometers (Fisher Scientific) in the range 0 → 6 and 6 → 30 cp.

Figure 3 shows the structural formulae of the two dyes JA120 and JA53 which we have used. Both JA120 and JA53 have similar absorption and fluorescence spectra (peaking at ≈ 645 and 672 nm and 650 and 690 nm, H_2O/*p*H 7, respectively) and similar

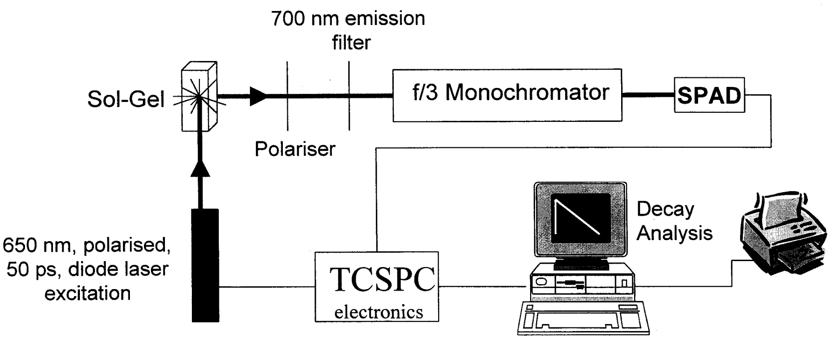

Figure 2. Instrumentation for measuring fluorescence anisotropy decays. SPAD – single photon avalanche diode.

Table 1. Compositions of sol–gels studied.

Excess acid normality in sol–gel, N, at *p*H	Final % SiO_2 in sol–gel (w/w)	t_g of pure sol (min)	Dilution/ doping of sol–gel	t_g of doped sol–gel	Probe	Refer to figure
0·25, 0·90	12·70	240–270	–	–	JA120	5
0·35, 0·76	15·11	48–55	½ sol, ½ H_2O	21 ± 1 h	JA120	7
0·35, 0·76	15·11	48–55	½ sol, ½ D_2O	26 ± 1·5 h	JA120	7
0·37, 0·73	15·00	68–74	–	–	JA120	9
0·37, 0·73	15·00	68–74	–	–	JA53	9
0·29, 0·84	5·94	2803–3013	1 M NaCl	1823–1883	JA120	10
0·26, 0·89	5·92	2895–3045	1 M $NaNO_3$	2580–2640	JA120	10

– Sol–gel not doped.

JA120

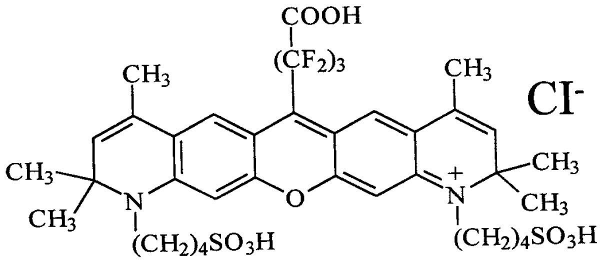

JA53

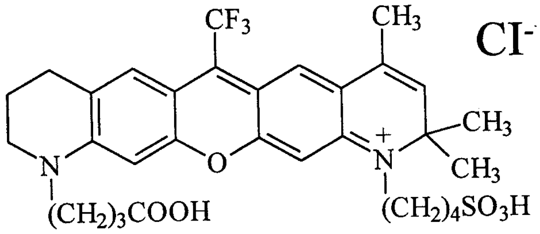

Figure 3. Structural formulae for JA120 and JA53. Cl^- – counter ion.

fluorescence lifetimes (≈ 1·83 ns and ≈ 1·76 ns, H_2O/*p*H 7, respectively). Near-infrared dyes are essential in this application in order not to excite intrinsic fluorescence from the sol and also reduce scatter from the particles and gel network. Although the dyes and silica particles are both cationic, the carboxylic acid functional group on each dye can undergo a diffusion controlled condensation reaction, (1), with a silanol group, Si–OH, leading to the gradual absorption of the dye by silica particles from the aqueous phase.

3. Theory and measurement principle

The theory of fluorescence anisotropy decay is well established in the study of bio and organic polymers and cellular membranes[4]. By recording vertically and horizontally polarised fluorescence decay curves, $F_V(t)$ and $F_H(t)$, orthogonal to vertically polarised and pulsed excitation, an anisotropy function $r(t)$ can be generated during measurement times short enough for negligible change in the sol–gel to occur (e.g. ≈ 2 min).

$$r(t) = F_V(t) - F_H(t)/F_V(t) + 2F_H(t). \tag{2}$$

For the case of a dye molecule bound to a silica particle $r(t)$ can be described well by the Brownian isotropic rotation of a sphere, giving the Perrin equation for the decay of fluorescence anisotropy[4]

$$r(t) = r_0 e^{-6Dt}, \tag{3}$$

where $r_0 = 0{\cdot}4$ is the initial anisotropy at $t = 0$ and, in the simplest case, the rotational correlation time t_r is described by the Stokes–Einstein equation

$$tr = \frac{1}{6D} = \frac{hV}{kT}, \tag{4}$$

where h is the microviscosity, V the particle hydrodynamic volume, T temperature and k Boltzmann constant.

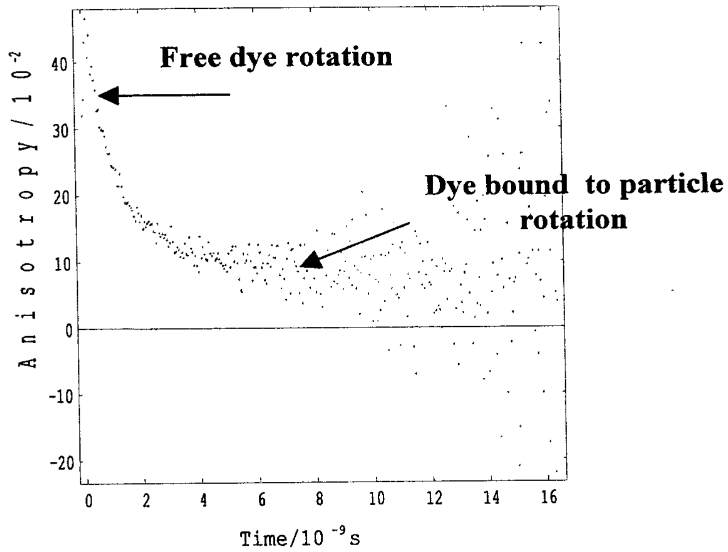

Figure 4. Typical fluorescence anisotropy decay in a silica sol measured in ≈ 2 min using TCSPC.

In recent studies[5,6] we have used a cationic dye JA120 (a xanthene type dye similar to rhodamine 6G but one of a series designed to fluoresce in the near-infrared[7]) which does not bleach like many dyes do, under strongly acidic conditions. For a silica sol at pH < 1 i.e. slightly positive surface charge, this slight repulsion of the dye by the silica leads to a fraction $\boldsymbol{f}$ of the total fluorescence being due to the probe molecules bound to silica particles and hence $\mathbf{1}-\boldsymbol{f}$ due to probe molecules unbound in the sol. The anisotropy then takes the form,

$$r(t) = (\mathbf{1}-\boldsymbol{f})r_0\exp(-t/\mathrm{t}_{r1}) + \mathbf{f}r_0\exp(-t/\mathrm{t}_{r2}). \qquad (5)$$

Fitting the anisotropy decay data to equation 5 shows that $\boldsymbol{f}$ increases with time as more dye is taken up by the silica particles. This was confirmed by precipitating out the silica by adding methanol, which revealed the dye to be both free in solution and attached to silica with more dye recovered in the methanol filtrate at earlier times. The initial anisotropy r_0 remained reassuringly constant at ~ 0·4 as $\boldsymbol{f}$ varied. A single anisotropy decay measurement, such as that shown in figure 4, gives t_{r1} and t_{r2}. Equation 4 can first be used with t_{r1} and the radius of the dye (found from studies in different solvents to be ≈ 7·5 Å for JA120 and ≈ 6·0 Å for JA53) to give the microviscosity of the aqueous phase of the sol and then used again with t_{r2} to give the particle size, quoted as radii in this paper. Extension of (5) to allow for a fraction of fluorescence $\boldsymbol{g}$, due to dye bound in the gel, just introduces another term $\boldsymbol{g}r_0$.

4. Results

It can be seen from figure 5 that the resolution we obtain, using JA120 as a probe, as the particles grow during polymerisation is close to 1 Å i.e. at least as good as X-ray and neutron scattering, but at much lower cost, greater convenience and simplified measurement. Also, unlike these other techniques, fluorescence anisotropy decay provides the microviscosity and particle measurements *in situ* at high silicate concentrations, even after the gel has formed. Also, the dye may be expected to intercalate within the ramified structures thought to describe the silica particles, contributing little to the overall hydrodynamic radius. The particle growth shown in figure 5 is as follows:

$$r \sim r_0 + (r_{\max} - r_0)(1 - e^{-kt}), \qquad (6)$$

where r is the particle radius (nm), $r_{\max}$ is the maximum particle radius (nm), r_0 the initial particle radius and k the rate constant for particle growth due to aggregation (s^{-1}). The k value for the data shown in figure 5 is $8{\cdot}6{*}10^{-5}\ \mathrm{s}^{-1}$.

A new aspect revealed by figure 5 is the peak after ≈ 2000 min. We attribute this to the intra-particle condensation rate (≈ $6{\cdot}0{*}10^{-6}\ \mathrm{s}^{-1}$ assuming an exponential reduction in particle radius) dominating the growth rate as the particle number density decreases. Shrinkage due to condensation (1) in a bulk gel is called syneresis and is well-known[1], but until our recent work[5,6] had not been reported at the particle level. This is perhaps due to the limitations of scattering techniques for studying particles against a background of scattering from the gel. Ignoring particle syneresis may prove to be a major omission in current theoretical models.

The sequence of events leading up to the formation of silica gel at low pH, revealed by our measurements is summarised in figure 6. Initially a few tetrahedra of monosilicic

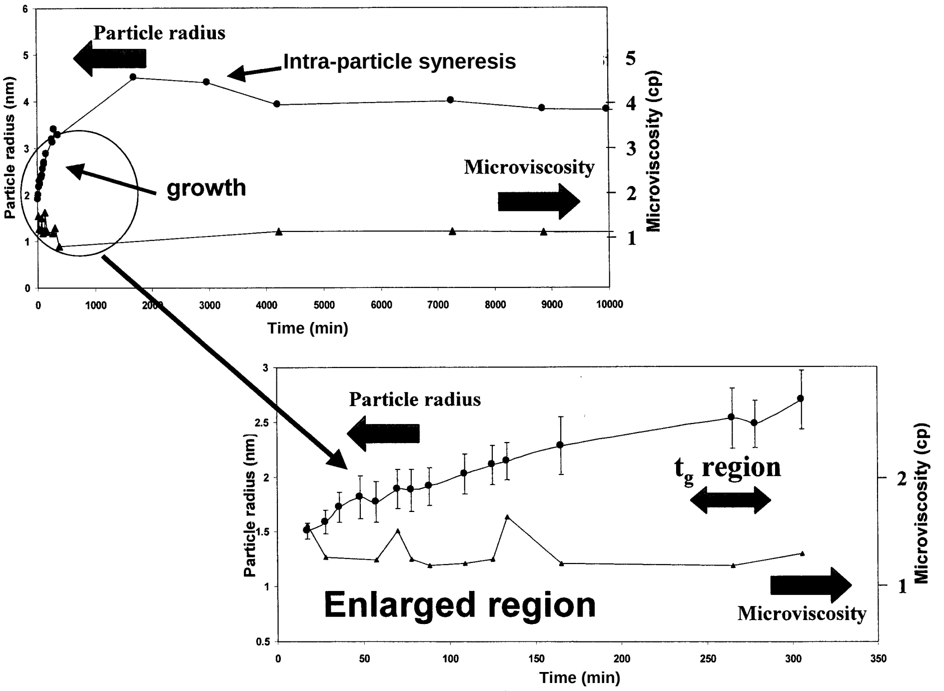

Figure 5. Typical silica particle radii and sol microviscosity across the sol-to-gel transition at t_g, for a 12·70% SiO_2 (final w/w) sol–gel, with an excess acid pH of 0·9. For this data the growth rate constant $k = 8{\cdot}6{*}10^{-5}\ s^{-1}$.

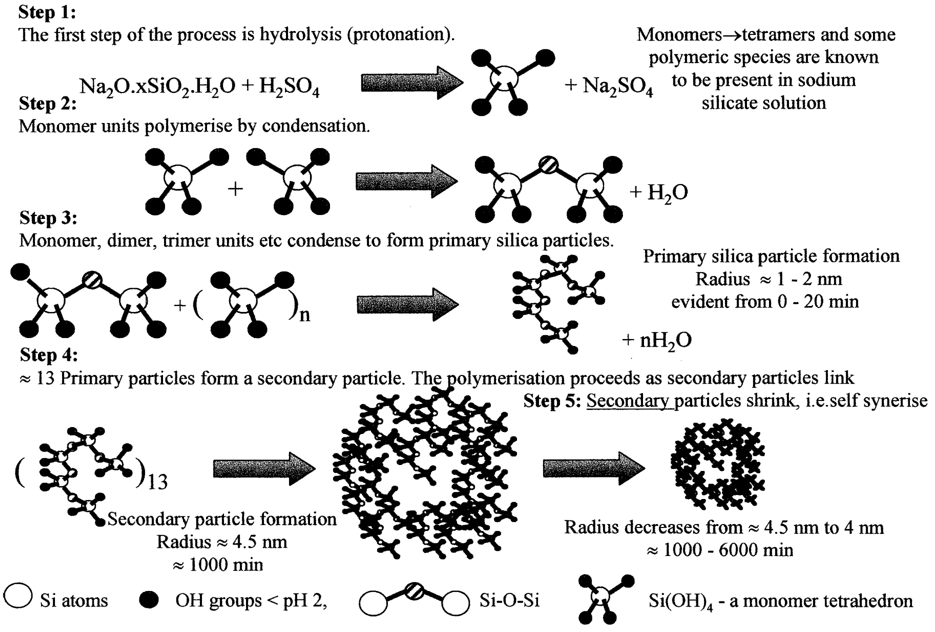

Step 1:
The first step of the process is hydrolysis (protonation).

$Na_2O.xSiO_2.H_2O + H_2SO_4$ → $+ Na_2SO_4$

Monomers→tetramers and some polymeric species are known to be present in sodium silicate solution

Step 2:
Monomer units polymerise by condensation.

$+ H_2O$

Step 3:
Monomer, dimer, trimer units etc condense to form primary silica particles.

$+ nH_2O$

Primary silica particle formation
Radius ≈ 1 - 2 nm
evident from 0 - 20 min

Step 4:
≈ 13 Primary particles form a secondary particle. The polymerisation proceeds as secondary particles link

Secondary particle formation
Radius ≈ 4.5 nm
≈ 1000 min

Step 5: Secondary particles shrink, i.e.self synerise

Radius decreases from ≈ 4.5 nm to 4 nm
≈ 1000 - 6000 min

Figure 6. The sequence of events leading up to silica hydrogel formation at low pH.

acid, $Si(OH)_4$, are joined together through siloxane (–Si–O–Si–) bonds formed in the condensation reactions (1) to give primary particles of mean radius ~ 1·5 nm. These primary particles diffuse through the sol, collide and bond together by means of siloxane bonds formed through more condensation reactions. Secondary particles are thus formed through aggregation until a maximum mean radius of ~ 4·5 nm is formed. A simple volume calculation predicts the secondary particles to be composed of a maximum of ~ 13 primary particles. The aggregation rate eventually slows as the free particle number density decreases and there are few external hydroxyl groups available for collisions to result in further bonding between particles. The intra-particle condensation rate then dominates over the aggregation rate as internal hydroxyl groups continue to condense (1) to form siloxane bonds, explaining the decrease observed from 4·5 nm to 4 nm. Eventually all but any sterically hindered internal hydroxyl groups are used up. In a nutshell, what we are observing here for the first time is what could be called microgelation or *intra*-particle syneresis. The usefulness of the silica particle growth curve shown in figure 5 from an industrial viewpoint lies in the fact that stopping the polymerisation process at a known particle radius leads to quality control of the surface area. From a theoretical viewpoint the growth curve provides new data for developing dynamical models, which in turn might lead to optimisation of the sol–gel process in general.

Another important feature of figure 5 is the near constancy of the microviscosity at ~ 1 cp, i.e. that of water even though the bulk viscosity is known to increase dramatically just prior to t_g. The primary particle hydrodynamic radius is slightly greater than that reported for silica gel[9,10] using small angle X-ray scattering, suggesting that water bound to the particles contributes to the hydrodynamic radius under these conditions (i.e. *p*H etc). The effect of hydrogen bonded water on silica hydrogel polymerisation is an uncharted area which we have been able to study using D_2O to disrupt hydrogen bonding.

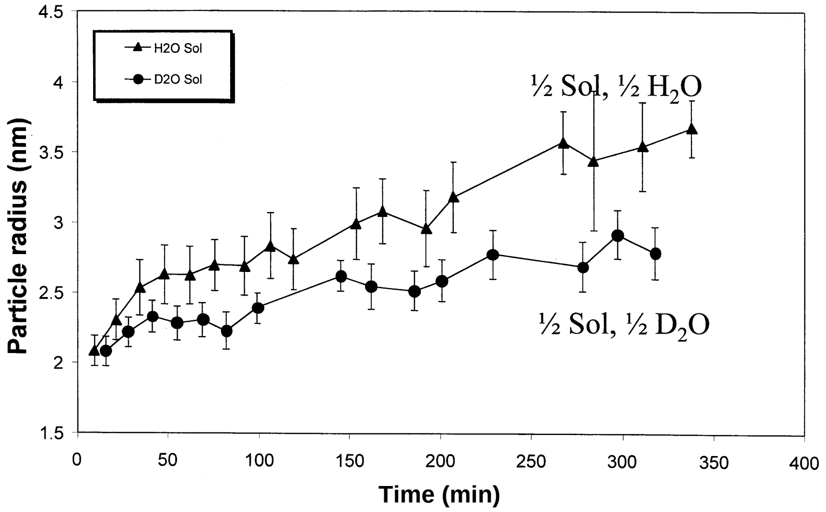

Figure 7. Silica particle growth in the absence and presence of D_2O. Errors in silica particle radii were calculated from three times the standard deviation of the bound dye rotational correlation time, t_{r2}.

Figure 7 shows particle growth in the absence and presence of the addition of an equal volume of D_2O or H_2O to an equal volume of 15·11 % SiO_2 (final w/w) sol–gel with an excess acid *p*H of 0·76. The corresponding t_g values were ≈ 26 ± 1·5 and 21 ± 1 h for the D_2O and H_2O additions respectively. The t_g of the undiluted sol was 48–55 min. The addition of D_2O is seen to reduce the hydrodynamic radius, which could be caused by a reduction in hydrogen bonding on adding D_2O, corresponding to ≈ 2–3 water molecules, solubility differences during early ripening, or the microviscosity differences of the sol (1·26 cp for H_2O addition as compared to 1·59 cp for D_2O addition) influencing the relative diffusion rates of silica particles. Figure 8 shows that the fluorescence kinetics in terms of rate of take up of the dye JA120 as reported by **f** is the same in the absence and presence of D_2O.

Figure 9 shows a comparison of the growth functions for a 15·00% SiO_2 (w/w) sol–gel, *p*H 0·73, 0·37 N excess acid, (t_g ≈ 68–74 min) using both JA120 and JA53 as a probe.

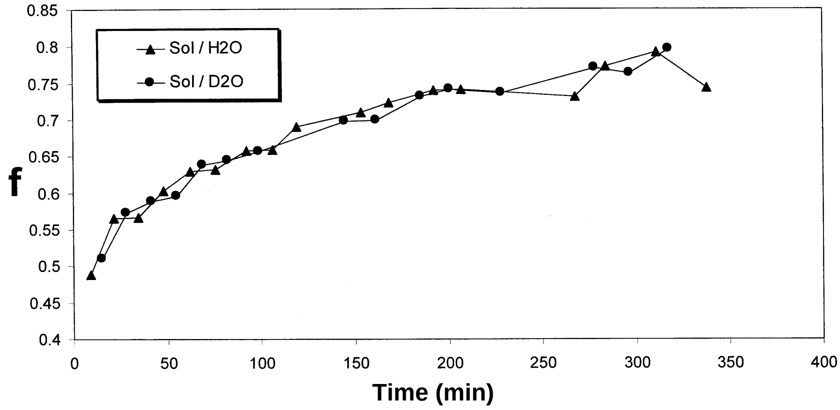

Figure 8. Fluorescence fraction, **f**, due to JA120 bound to silica particles in the absence and presence of D_2O.

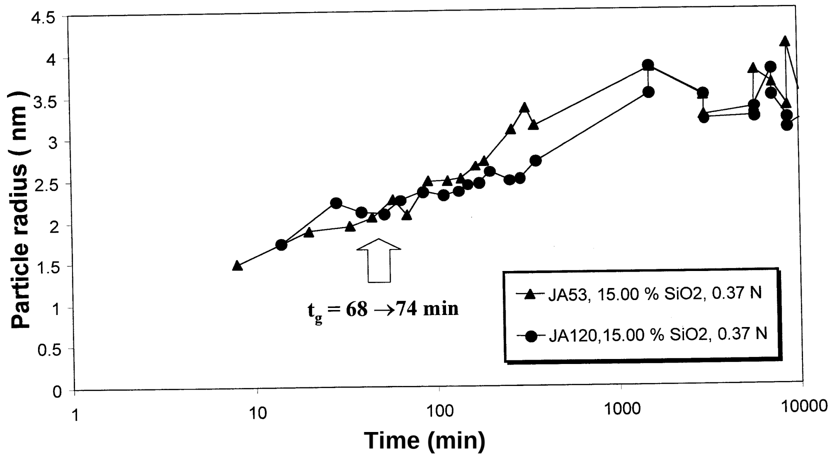

Figure 9. Comparison of silica particle growth curves as sensed by JA120 and JA53.

Table 2. Effect of inorganic salt addition on the parameters of (6). r_0 – Initial silica particle radius, k – initial aggregate growth rate (the linear regression coefficient R^2 was better than 0·97 for all the above data), t_g – macrogelation time (the time for the liquid, the 'sol', to set firm)

Sol–gel/added salts	r_0 (nm)	k (s^{-1})	t_g (min)
[a]5·94% SiO_2, 0·29 N (pure sol)	1·81 ± 0·05	2·36e^{-5}	2803–3013
5·94% SiO_2, 0·29 N (0·1 M NaCl)	1·77 ± 0·02	3·36e^{-5}	2743–2833
5·94% SiO_2, 0·29 N (1 M NaCl)	1·69 ± 0·15	3·94e^{-5}	1823–1883
[a]5·92% SiO_2, 0·26 N (pure sol)	1·70 ± 0·04	2·27e^{-5}	2895–3045
5·92% SiO_2, 0·26 N (0·1 M $NaNO_3$)	1·71 ± 0·03	2·25e^{-5}	2820–2910
5·92% SiO_2, 0·26 N (1 M $NaNO_3$)	1·70 ± 0·03	2·45e^{-5}	2580–2640
5·92% SiO_2, 0·26 N (0·1 M NaF)	–	–	≈ 8

[a]Both the 5·94% SiO_2, 0·29 N and the 5·92% SiO_2, 0·26 N sol–gels can be considered equivalent for comparison purposes.

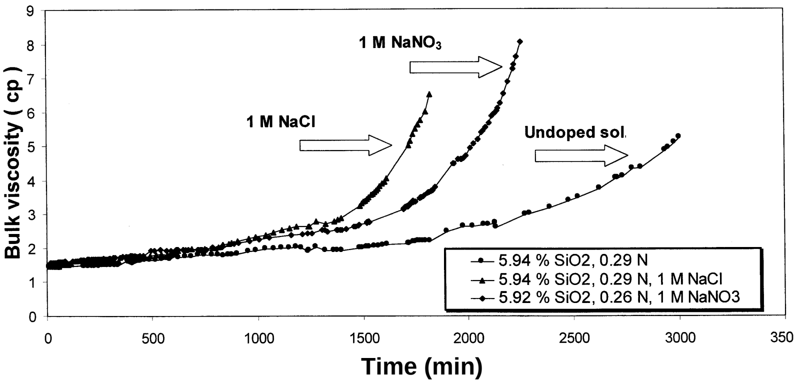

Figure 10. The effect on the bulk viscosity and hence t_g by adding inorganic salts. 1 M $NaNO_3$ and 1 M NaCl sols were prepared by adding 4·25 g and 2·92 g of the respective salts to 50 ml of sol containing 10^{-5} M JA120. Bulk viscosities were recorded using Ostwald viscometers.

The results for both dyes are self consistent. Clearly, the smallest silica particle size which is measurable is determined by the dye dimensions, though at ≈ 4 nm particle radius, the dyes we have used contribute < 1% to the total hydrodynamic volume.

We sought to test fluorescence anisotropy metrology further by adding salts to the initial sol and noting the effect on particle size. The addition of salts is well-known to reduce t_g due to the change in sol ionic strength which reduces the surface charge and mutual repulsion of silica particles and hence increases the *inter*-particle condensation reaction rate. Figure 10 shows the effect on the bulk viscosity by the addition of NaCl and $NaNO_3$ as compared to the original sol. Table 2 shows the effect on the kinetic parameters of equation 6 by adding NaCl and $NaNO_3$. Little change in the initial primary particle radius of ≈ 1·7 nm was observed. There is little change in the growth rate k even though t_g changes quite markedly on the addition of salt. The addition of NaF produced rapid gelation which was too quick to be studied.

5. Conclusions

Fluorescence anisotropy metrology has been shown to offer near Å resolution of the effect of changes in the formation dynamics of the silica particle clusters which are responsible for producing sol to gel transitions. The *in-situ* nature of such measurements should provide a more stringent test of dynamical models and offer a practical method of controlling important production parameters for silica gel such as surface area, porosity and density etc.

Acknowledgements

The authors would like to thank the Engineering & Physical Science Research Council, Swindon and Crosfield Ltd, Warrington for financial support and Dr Jutta Arden-Jacob for kindly donating samples of JA120 and JA53.

References

1. Brinker C J and Scherer G 1989 *Sol–gel science, the physics and chemistry of sol–gel processing* (San Diego: Academic Press)
2. Thompson N L 1991 In *Topics in fluorescence spectroscopy* (ed.) J R Lakowicz (New York: Plenum) vol 1, pp 337
3. Birmingham J J, Hughes N P and Treloar R 1995 *Philos. Trans. R. Soc. London B* **350** 325
4. Lakowicz J R 1999 *Principles of fluorescence spectroscopy* 2nd edn (New York: Plenum)
5. Geddes C D, Birch D J S, Apperson K, Chevers J M and McKeown I P 1999 *SPIE Proc.* **3602** 75
6. Geddes C D and Birch D J S 2000 *J. Non-Cryst. Solids* **270** 191
7. Arden-Jacob J, Marx N J and Drexhage K H 1997 *J. Fluoresc.* **7** 91
8. Birch D J S and Imhof R E 1991 In *Topics in fluorescence spectroscopy* (ed.) J R Lakowicz (New York: Plenum) vol 1, pp 1
9. Himmel B, Gerber T H and Bürger H 1987 *J. Non-Cryst. Solids* **91** 122
10. Gerber T H, Himmel B and Hübert C 1994 *J. Non-Cryst. Solids* **175** 160